SUPPORTING INFORMATION

Influence of C–H/X (X = S, Cl, N, Pt/Pd) interactions on the molecular and crystal structures of Pt(II) and Pd(II) complexes with thiomorpholine-4-carbonitrile: crystallographic, thermal and DFT study

Predrag Ristić[a], Vladimir Blagojević[b], Goran Janjić[c], Marko Rodić[d], Predrag Vulić[e], Morgan Donnard[f], Mihaela Gulea[g], Agnieszka Chylewska[h], Mariusz Makowski[h], Tamara Todorović[a], Nenad Filipović[i,*]

[a] *University of Belgrade - Faculty of Chemistry, Studentski trg 12-16, 11000 Belgrade, Serbia*

[b]*Institute of Technical Sciences of the Serbian Academy of Sciences and Arts, Knez Mihailova 35/IV, 11000 Belgrade, Serbia*

[c]*Institute of Chemistry, Metallurgy and Technology, University of Belgrade, Njegoševa 12, 11000 Belgrade, Serbia*

[d]*Department of Chemistry, Faculty of Sciences, University of Novi Sad, Trg Dositeja Obradovića 4, 21000 Novi Sad, Serbia*

[e]*Faculty of Mining and Geology, University of Belgrade, Đušina 5, 11000 Belgrade, Serbia*

[f]*Université de Strasbourg, Université de Haute-Alsace, CNRS, LIMA – UMR 7042, ECPM, 67000 Strasbourg, France*

[g]*Université de Strasbourg, CNRS, LIT – UMR 7200, Faculty of Pharmacy, 67000 Strasbourg, France*

[h]*Faculty of Chemistry, University of Gdansk, Wita Stwosza 63, PL80-308 Gdansk, Poland*

[i] *University of Belgrade - Faculty of Agriculture, Nemanjina 6, 11000 Belgrade, Serbia*

*Corresponding author: Nenad Filipović, PhD, Associate Professor, University of Belgrade - Faculty of Agriculture, Nemanjina 6, 11000 Belgrade, Serbia; E-mail: nenadf@agrif.bg.ac.rs

SUPLEMENTARY FIGURES AND SCHEMES

Figure S1. IR spectra of gaseous decomposition products obtained during TG experiments with **1**(A) and **2** (B).

Figure S2. The 3D presentation of thermal decompositions *versus* time together with IR spectra of their gaseous products: (a) **1**; (b) **2**.

Figure S3. Overlapped experimental (blue) and calculated (red) powder XRD diffractograms of 1 (A) and 2 (B).

Figure S4. Comparison between experimental powder XRD patterns of **1** (left) and **2** (right) with simulated patterns of their analogues with different position of M–S bond with respect to the TM-CN ring chair conformation.

Figure S5. Optical microscope images of Pt- (left) and Pd-complex (right) showing as-obtained single crystals.

Figure S6. SEM images of Pt- (left) and Pd-complex (right) after reduction to powder for XRD measurements.

Figure S7. ^{1}H NMR spectra of TM-CN in DMSO-d_6 (A) and CD_3NO_2 (B).

Figure S8. ^{13}C NMR spectra of TM-CN in DMSO-d_6 (A) and CD_3NO_2 (B).

Figure S9. ^{1}H (A) and ^{13}C NMR (B) spectra of **1** in DMSO-d_6.

Figure S10. COSY spectrum of **1** in DMSO-d_6.

Figure S11. NOESY spectrum of **1** in DMSO-d_6.

Figure S12. ^{1}H–^{13}C HSQC spectrum of **1** in DMSO-d_6.

Figure S13. ^{1}H (A) and ^{13}C NMR (B) spectra of **1** in CD_3NO_2.

Figure S14. ^{1}H (A) and ^{13}C NMR (B) spectra of **2** in DMSO-d_6.

Figure S15. ^{1}H (A) and ^{13}C NMR (B) spectra of **2** in CD_3NO_2.

Scheme S1. Labelling of atoms used for NMR signal assignments.

SUPLEMENTARY TABLES

Table S1. Experimental vibrational frequencies (cm^{-1}) and signals description of complexes studied.

Table S2. Crystal data and structure refinement for **1** and **2**.

Table S3. Selected bond lengths (Å) and angles (°) for complexes **1** and **2**.

Table S4. Results of energy calculations for C-H/Cl-M, C-H/S-M, C-H/M and C-H/N≡C interactions (M= Pd(II) and Pt(II)) at *wb97xd/6-31+g** +lanl2dz* level of theory. Energies are expressed in kcal/mol.

Table S5. C-H/M interactions obtained from the periodic calculations of axial and equatorially coordinated Pd and Pt.

Table S6. ^{1}H NMR spectral data (399.74 MHz) in DMSO-d_6 and CD_3NO_2 at 298 K for TM-CN and complexes **1** and **2**.

Table S7. ^{13}C NMR spectral data (100.53 MHz) in DMSO-d_6 and CD_3NO_2 at 298 K for TM-CN and complexes **1** and **2**.

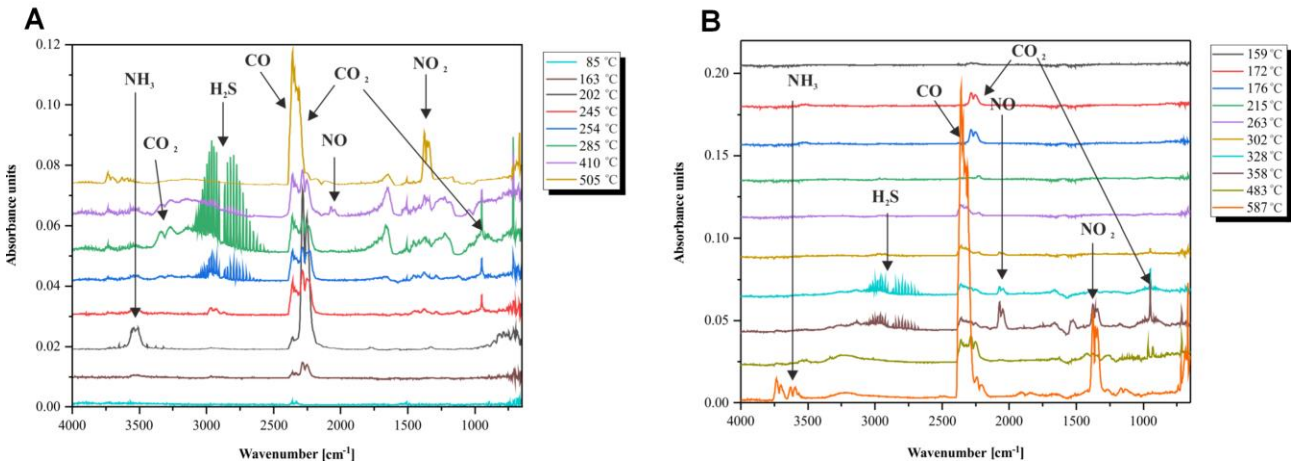

Figure S1. IR spectra of gaseous decomposition products obtained during TG experiments with **1**(A) and **2** (B).

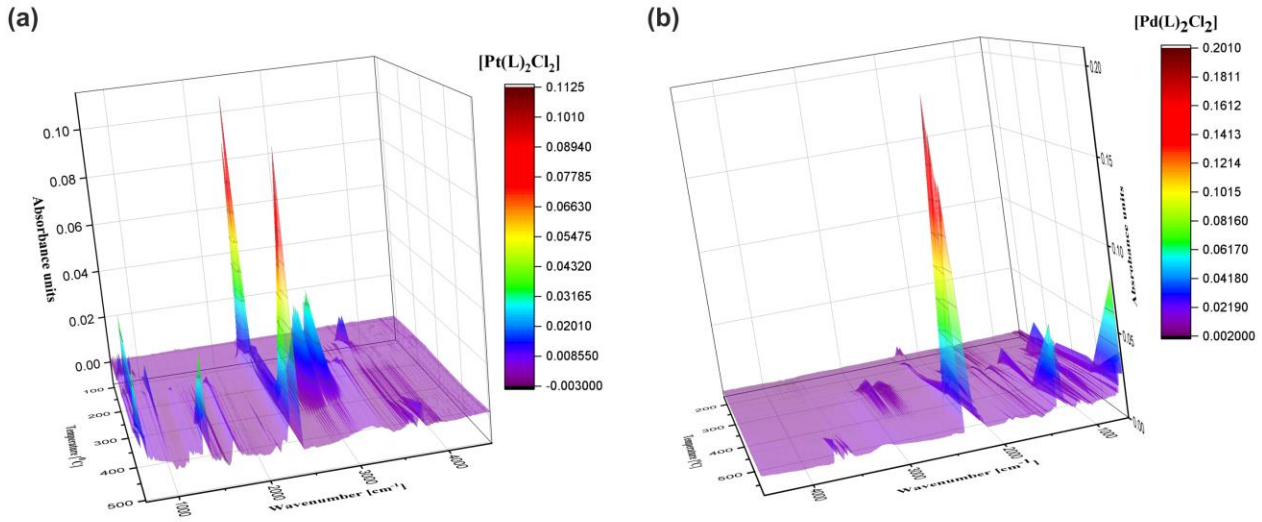

Figure S2. The 3D presentation of thermal decompositions *vs* time together with IR spectra of their gaseous products: (a) **1**; (b) **2**.

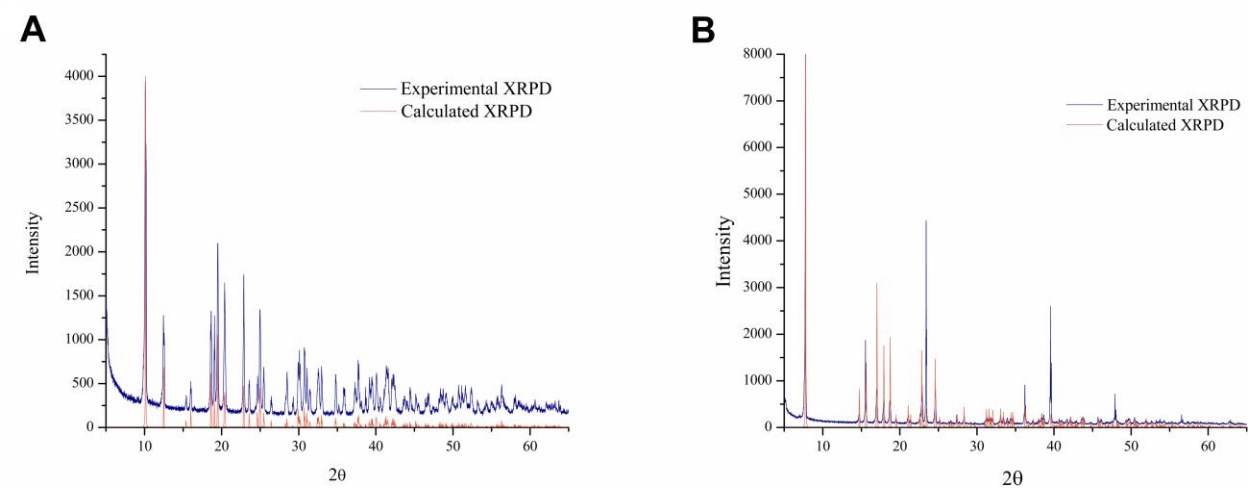

Figure S3. Overlapped experimental (blue) and calculated (red) powder XRD diffractograms of **1** (A) and **2** (B).

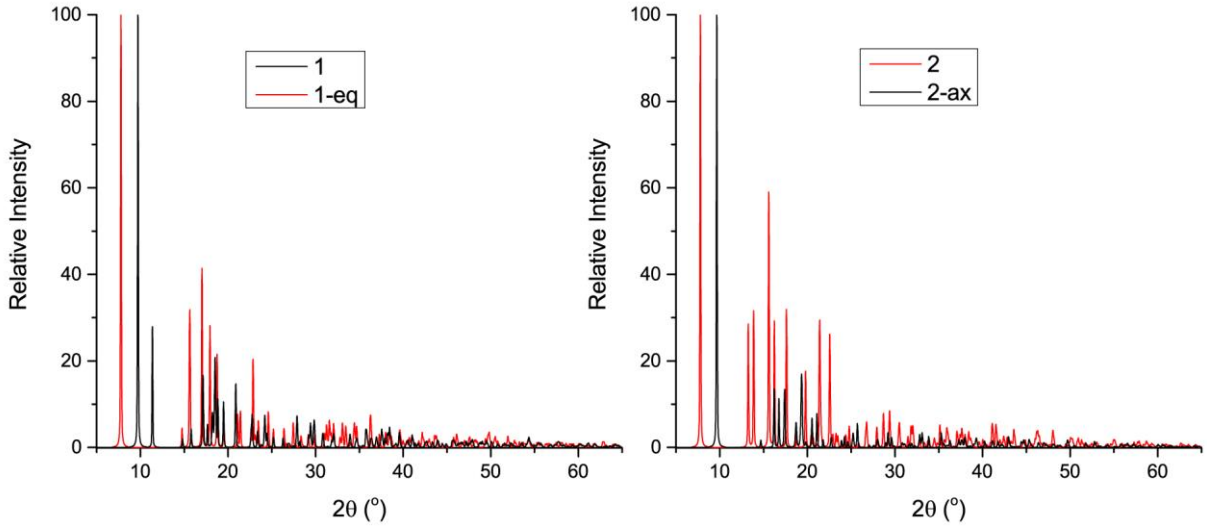

Figure S4. Comparison between experimental powder XRD patterns of **1** (left) and **2** (right) with simulated patterns of their analogues with different TM-CN conformation of metal-sulfur bond.

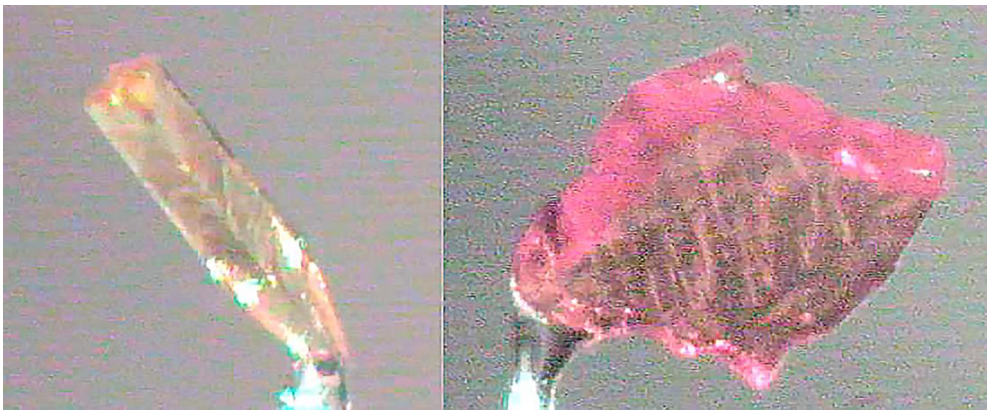

Figure S5. Optical microscope images of Pt- (left) and Pd-complex (right) showing as-obtained single crystals.

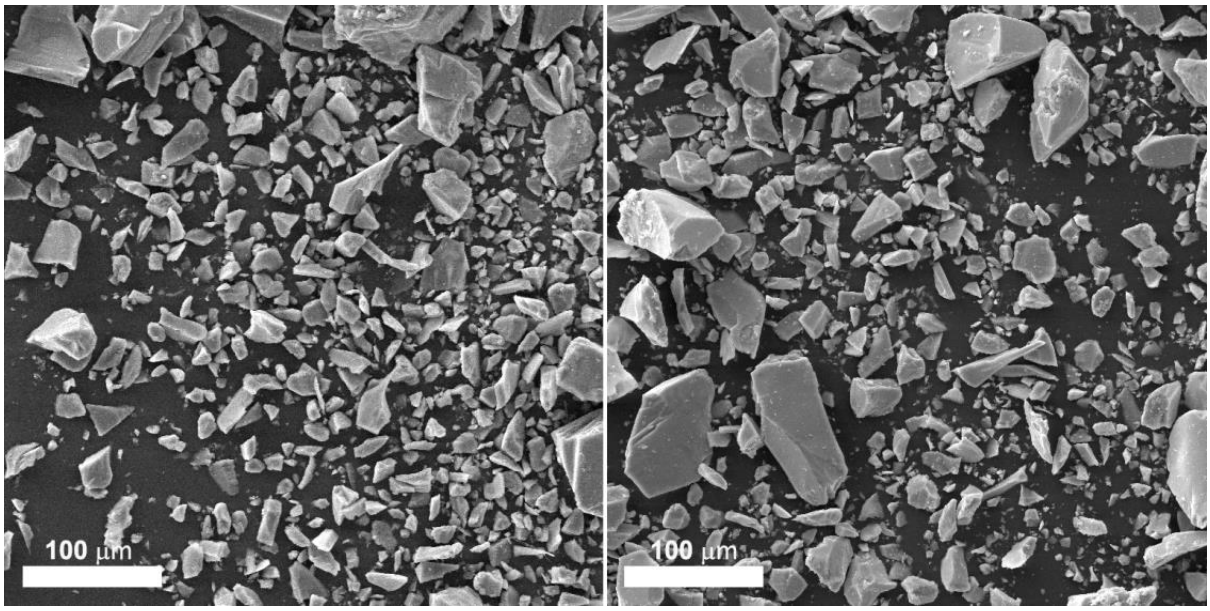

Figure S6. SEM images of Pt- (left) and Pd-complex (right) after reduction to powder for XRD measurements.

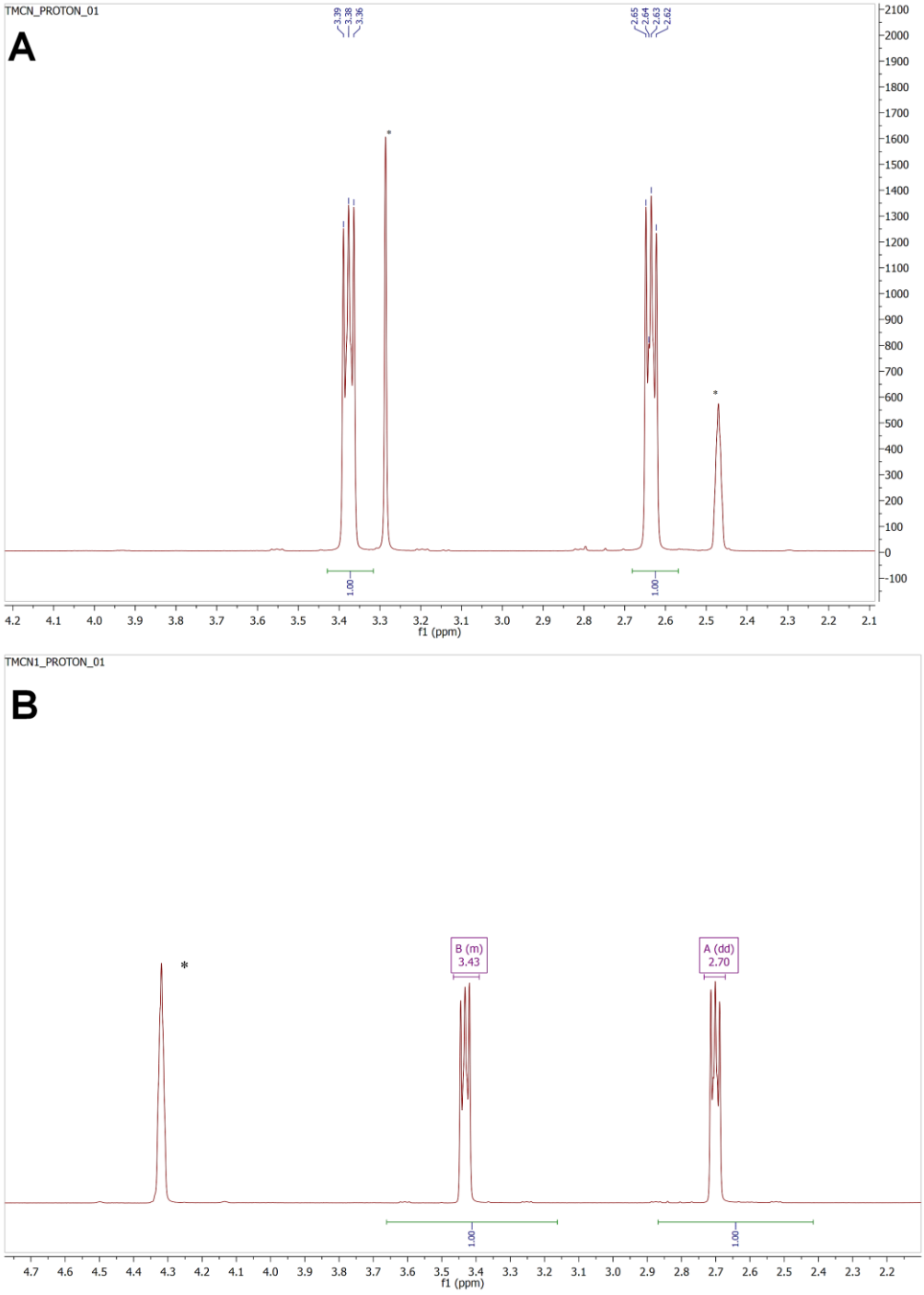

Figure S7. ^{1}H NMR spectra of TM-CN in DMSO-d_6 (A) and CD_3NO_2 (B).

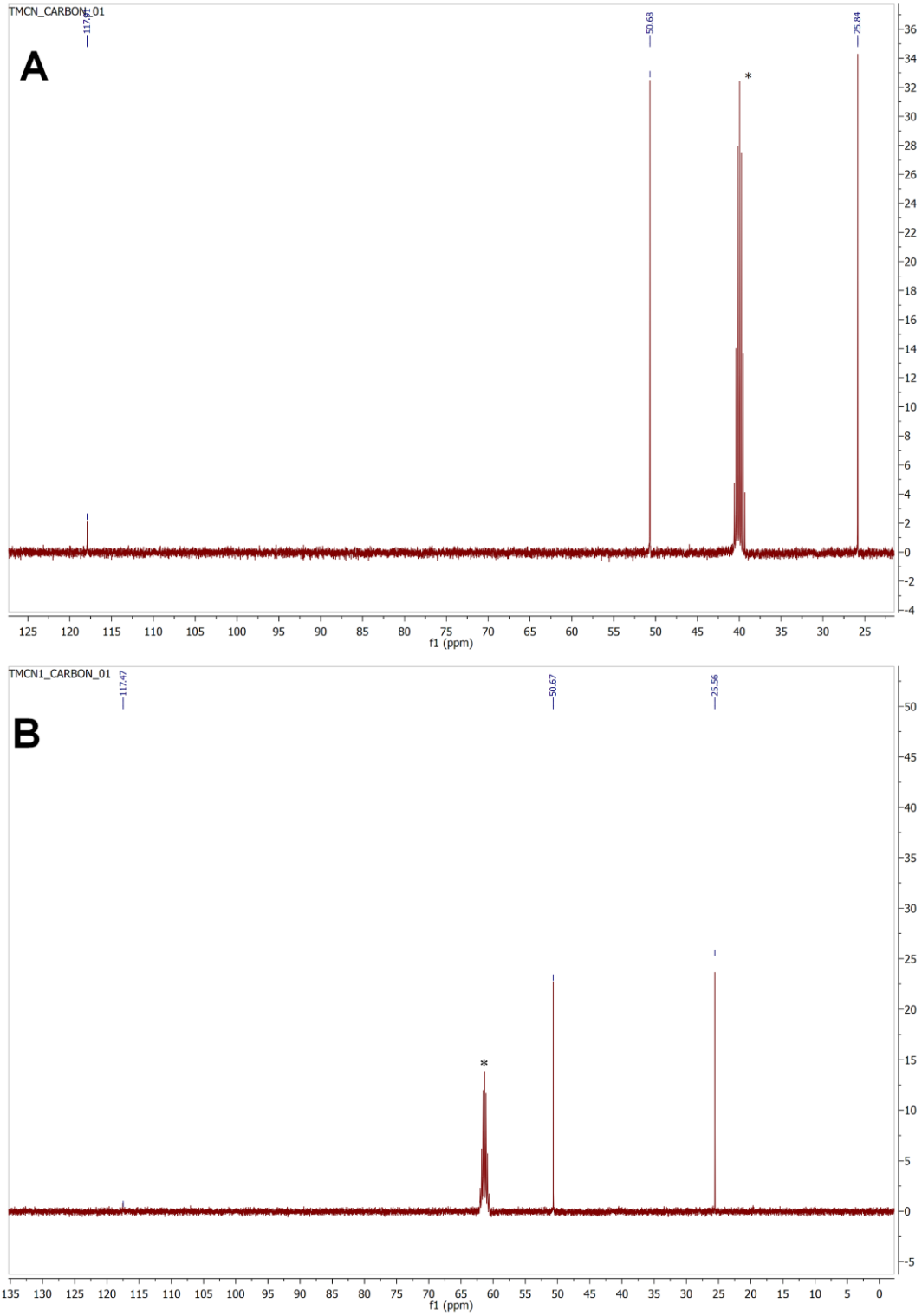

Figure S8. ^{13}C NMR spectra of TM-CN in DMSO-d_6 (A) and CD_3NO_2 (B).

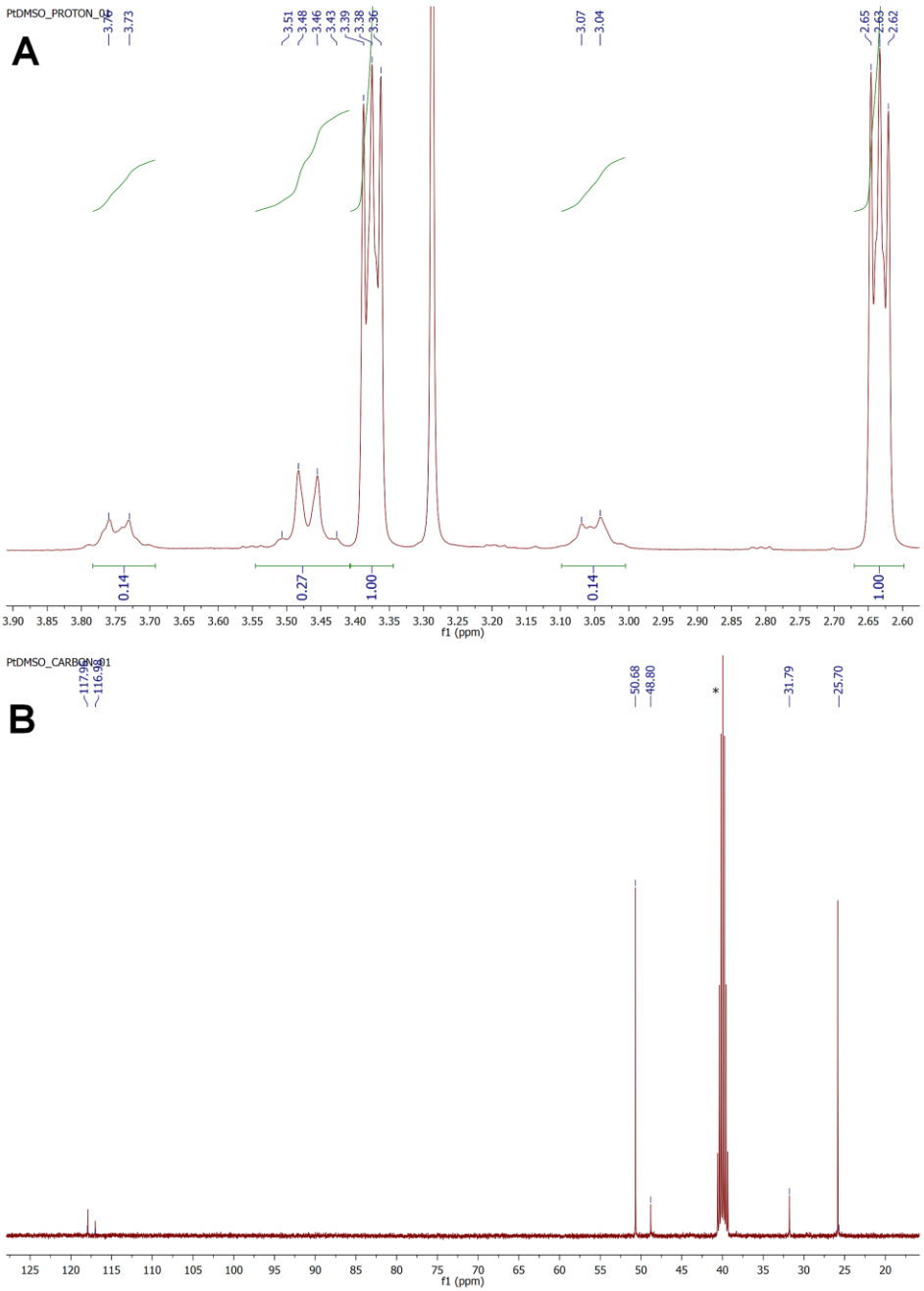

Figure S9. ^{1}H (A) and ^{13}C NMR (B) spectra of **1** in DMSO-d_6.

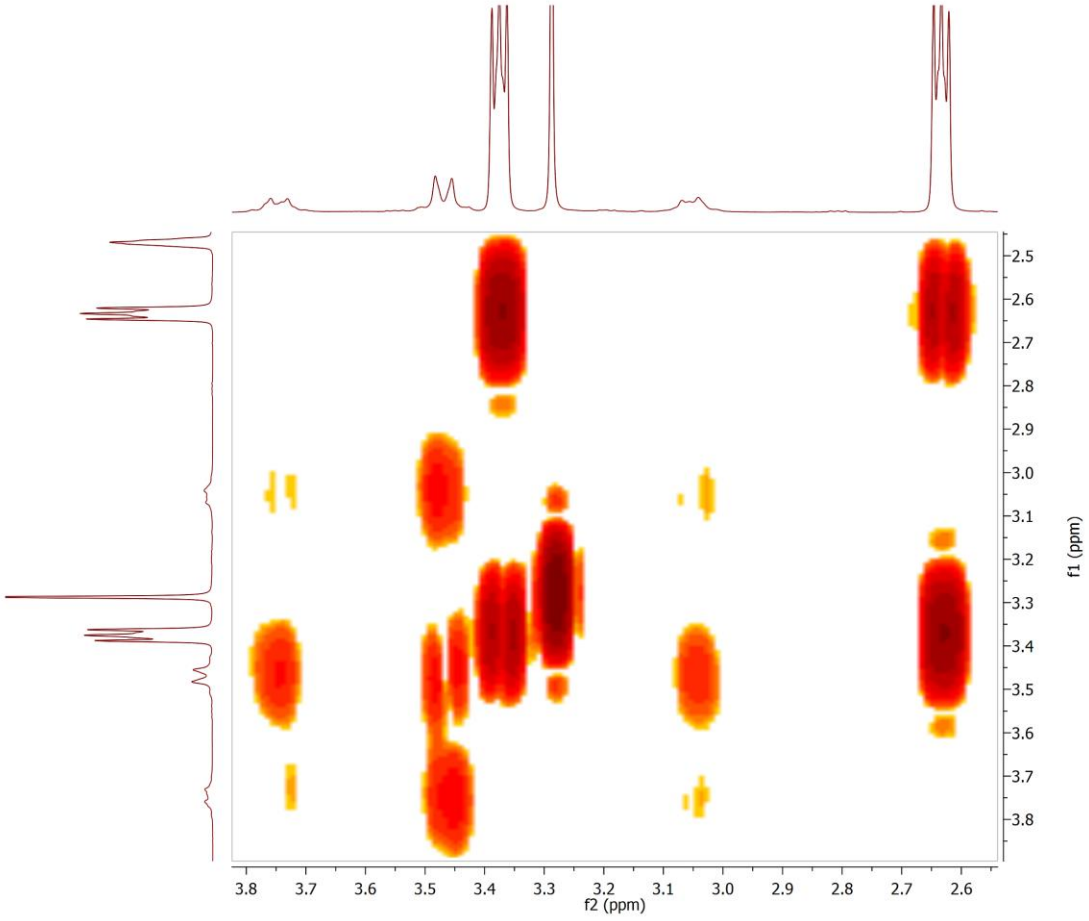

Figure S10. COSY spectrum of **1** in DMSO-d_6.

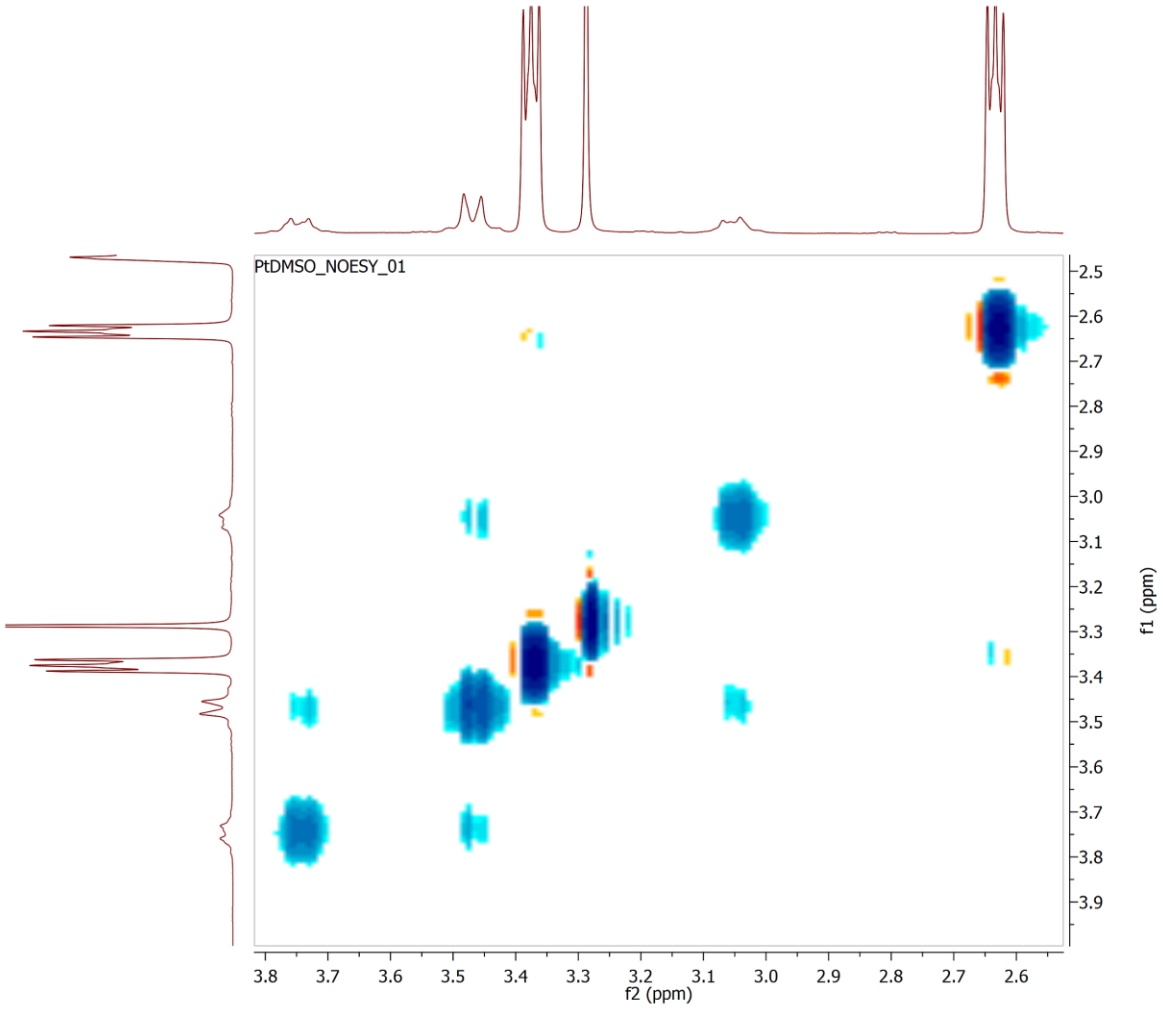

Figure S11. NOESY spectrum of **1** in DMSO-d_6.

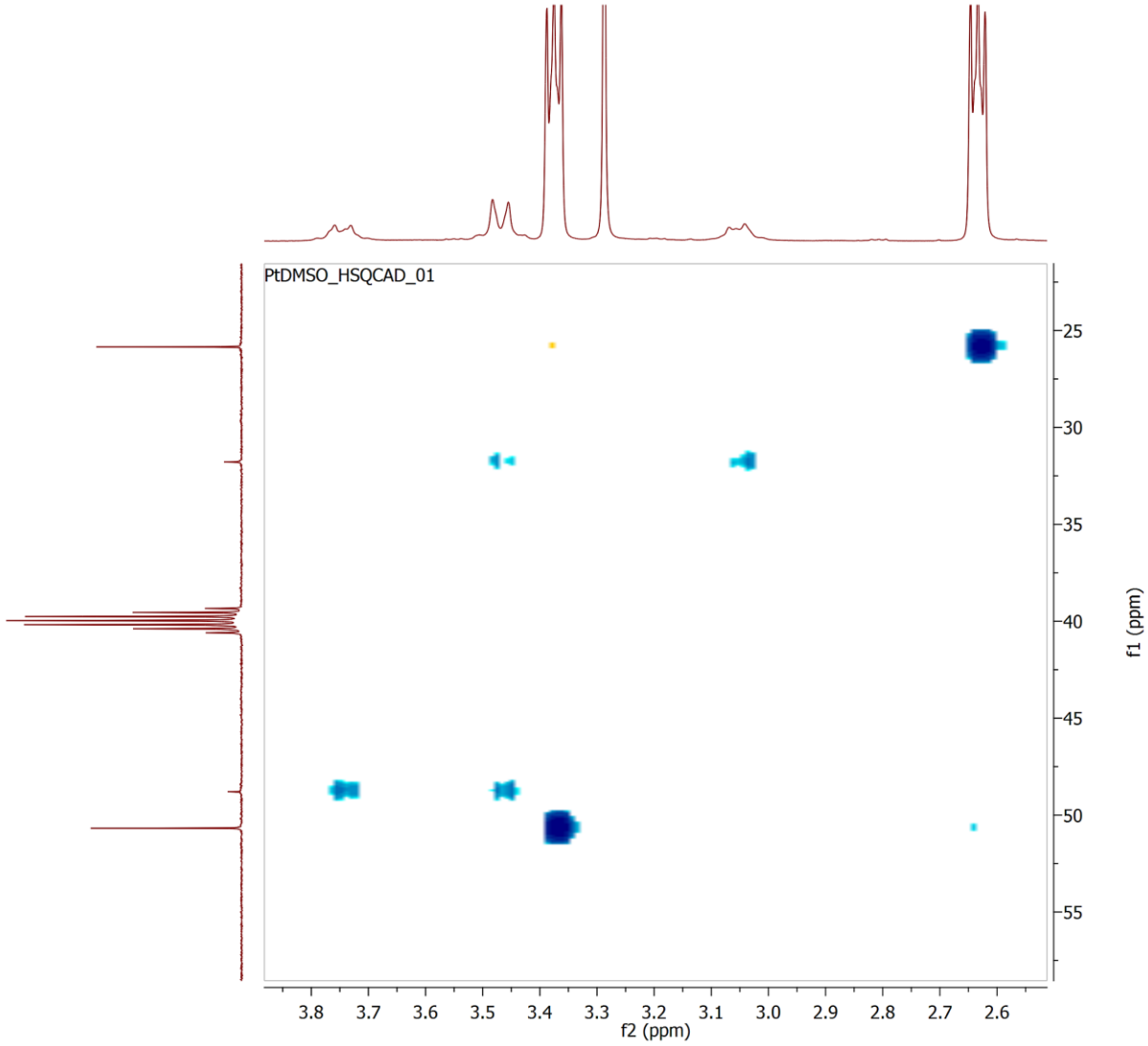

Figure S12. $^{1}H–^{13}C$ HSQC spectrum of **1** in DMSO-d_6.

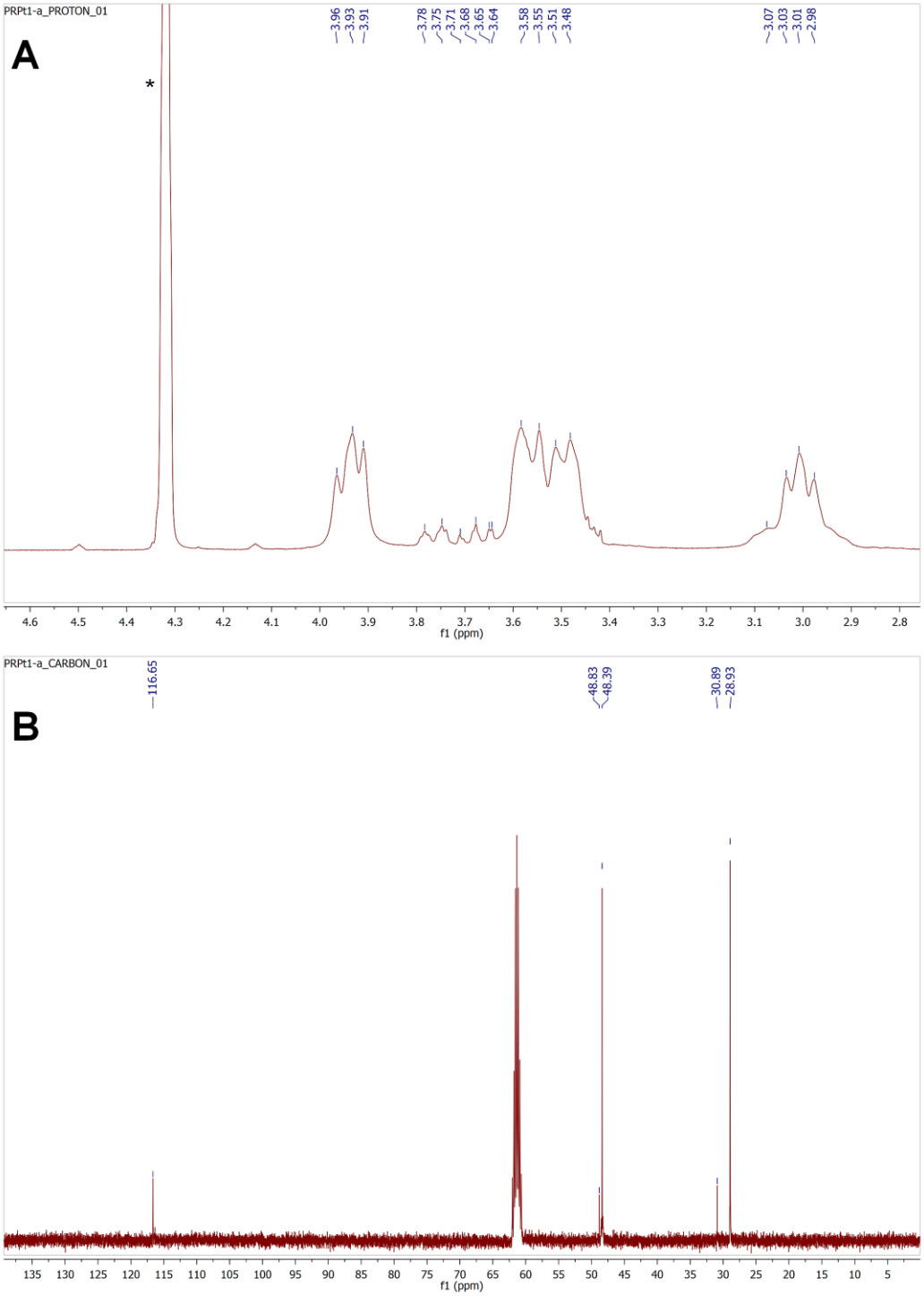

Figure S13. ^{1}H (A) and ^{13}C NMR (B) spectra of **1** in CD_3NO_2.

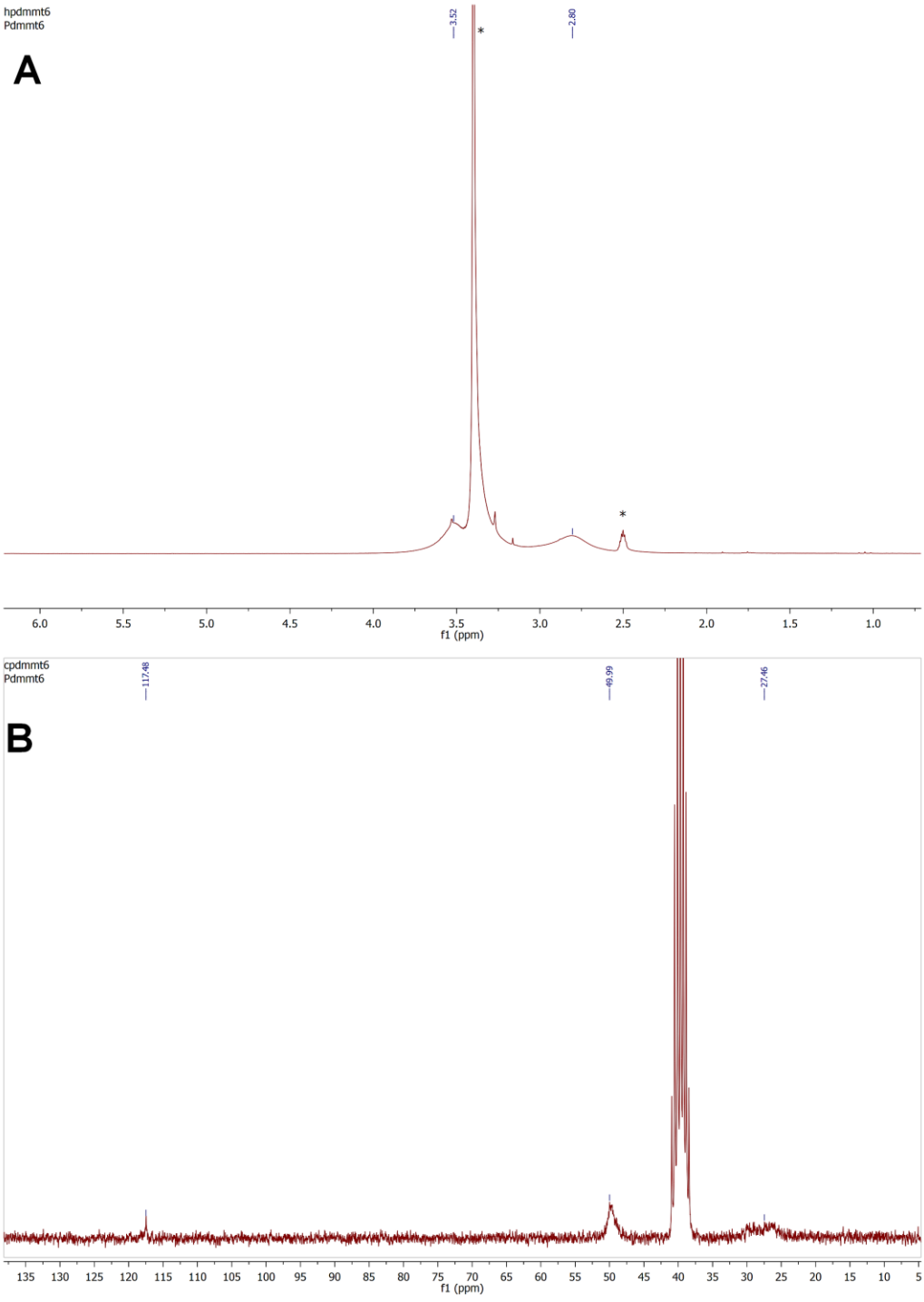

Figure S14. ^{1}H (A) and ^{13}C NMR (B) spectra of **2** in DMSO-d_6.

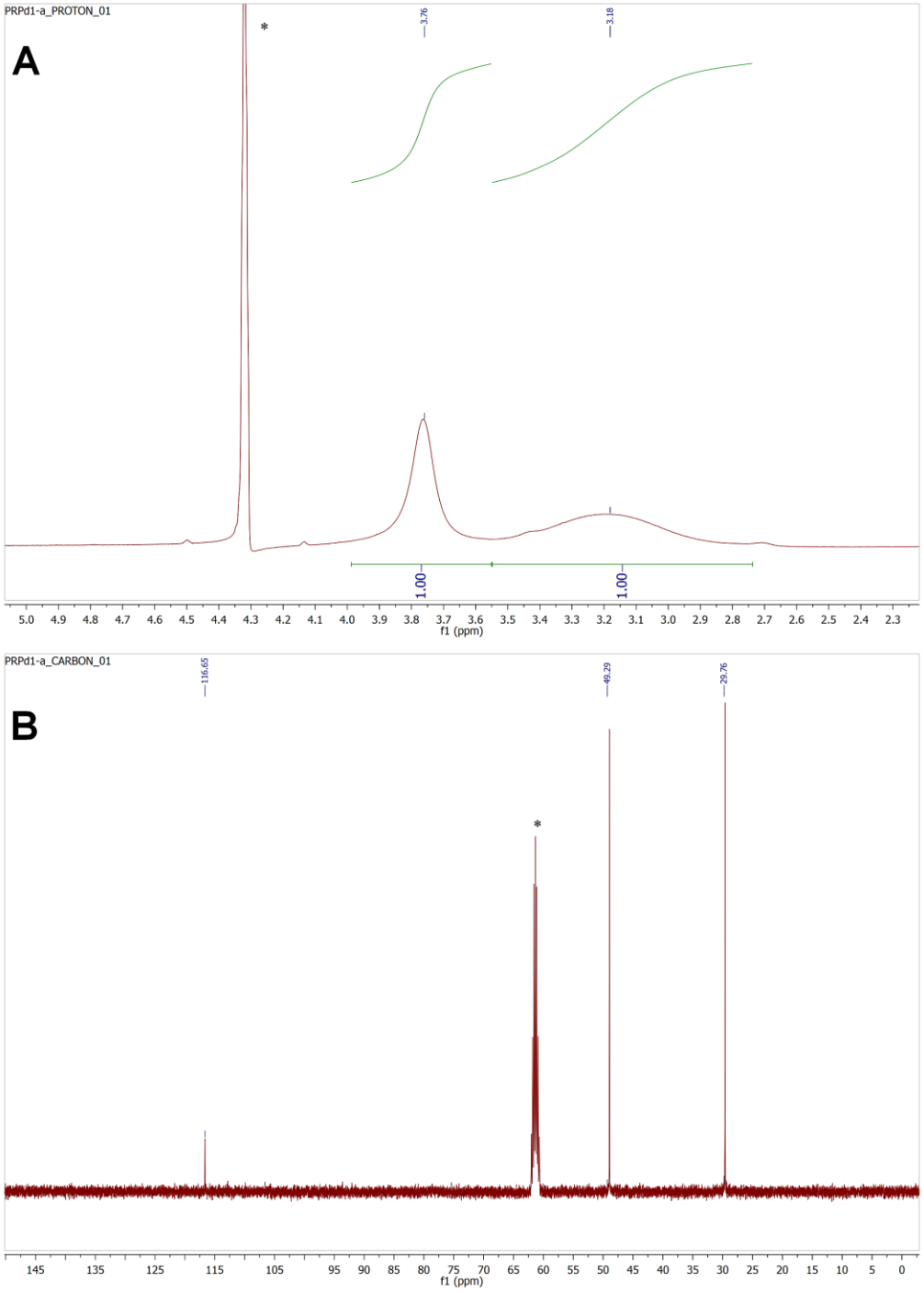

Figure S15. ^{1}H (A) and ^{13}C NMR (B) spectra of **2** in CD_3NO_2.

Table S1. Experimental vibrational frequencies (cm^{-1}) and signals description of complexes studied.

1			**2**		
UATR experimental frequency (cm^{-1})	**IR intensity (%)**	**Vibrational assignments**	**UATR experimental frequency (cm^{-1})**	**IR intensity (%)**	**Vibrational assignments**
3601 vw 3355 w	(92) (92)	*trans*-geometry	3461 vw 3354 w	(93) (93)	*trans*-geometry
2997 w	(91)		2995 ms	(90)	CH_2 sym
2980 w	(89)	CH_2 sym CH_2 asym	2925 vw	(93)	CH_2 asym
2916 vw	(91)		2263 ms	(88)	ν C≡N
2867 vw	(91)		2214 s	(80)	
2208 vs	(59)	ν C≡N	1649 ms	(89)	
1652 w	(93)		1597 ms	(89)	ν C-S
1598 w	(92)	ν C-S	1546 ms	(91)	
1454 s	(82)		1401 s	(81)	
1420 s	(79)		1277 s	(84)	ν C-C CH_2 wag CH_2 twist
1391 s	(74)		1197 mw	(88)	
1364 s	(78)		1166 mw	(86)	
1283 s	(82)		1113 mw	(87)	
1227 ms	(87)	ν C-C CH_2 wag CH_2 twist	1029 s	(85)	b C≡N
1197 ms	(87)		946 vs	(67)	
1176 ms	(83)		832 w	(91)	CH_2 rock
1147 ms	(82)		734 mw	(89)	
1120 s	(78)		648 mw	(89)	
1027 s	(79)	b C≡N	573 mw	(86)	
980 ms	(83)	CH_2 rock	543 mw	(85)	b NCN

1			2		
UATR experimental frequency (cm^{-1})	**IR intensity (%)**	**Vibrational assignments**	**UATR experimental frequency (cm^{-1})**	**IR intensity (%)**	**Vibrational assignments**
949 vs	(56)		504 s	(79)	ν Pd-S
726 ms	(88)		374 vw	(90)	
580 s	(84)		364 w	(84)	
540 ms	(88)	b NCN	355 vs	(56)	ν Pd-Cl
505 vs	(74)	ν Pt-S	333 s	(78)	
354 vs	(53)		319 vs	(28)	
347 vs	(25)	ν Pt-Cl			
339 vs	(10)				
321 vs	(22)				

Abbreviations used: ν = streching; b = bending; wag = wagging; twist = twisting; rock = rocking; sym = symmetric stretch; asym = asymmetric stretch; w = weak; m = medium; s = strong; ms = medium strong; vs = very strong; vw = very weak.

Table S2. Crystal data and structure refinement for **1** and **2**.

Compound	**1**	**2**
Molecular formula	$C_{10}H_{16}Cl_2N_4PtS_2$	$C_{10}H_{16}Cl_2N_4PdS_2$
Formula weight	522.38	433.69
Temperature (K)	294(2)	294(2)
Wavelength (Å)	0.71073	0.71073
Crystal system	Monoclinic	Monoclinic
Space group	*I* 2/*a*	*P* 2_1/*c*
a (Å)	9.9954(3)	11.4399(4)
b (Å)	11.0764(3)	7.0711(2)
c (Å)	14.8663(4)	9.5192(4)
β (°)	107.508(3)	96.179(4)
Volume ($Å^3$)	1569.64(7)	765.56(5)
Z	4	2
ρ_{calc} (Mg/m^3)	2.211	1.881
μ (mm^{-1})	9.537	1.82
F(000)	992	432
Crystal size (mm)	0.61 × 0.14 × 0.11	0.51 × 0.49 × 0.14
θ Range for data collection (°)	2.33 – 28.93	3.39 – 29.06
Reflections collected	7449	25252
Independent reflections	1903 [*R*(int) = 0.046]	3440 [*R*(int) = 0.070]
Absorption correction	Gaussian	Analytical
Refinement method	full-matrix least-squares on F^2	
Data/restraints/parameters	1903/0/89	3440/0/90
Goodness-of-fit on F^2	1.27	1.25
Final *R* indexes [$I > 2\sigma(I)$]	R_1 = 0.0327, wR_2 = 0.0802	R_1 = 0.0505, wR_2 = 0.1176
Final *R* indexes [all data]	R_1 = 0.0387, wR_2 = 0.0835	R_1 = 0.0551, wR_2 = 0.1211
Largest diff. peak and hole, e $Å^{-3}$	1.06 and –2.18	1.30 and –1.66

Table S3. Selected bond lengths (Å), bond angles (°) and torsional angles (°) for complexes **1** and **2**.

	1	**2**
M1[a]–Cl1	2.3059(11)	2.2981(9)
M1–S1	2.3135(10)	2.3121(9)
S1–C1	1.816(5)	1.823(4)
S1–C3	1.810(5)	1.808(4)
N1–C2	1.463(6)	1.471(6)
N1–C5	1.315(6)	1.317(6)
N1–C4	1.454(6)	1.452(6)
Cl1–M1–S1^{i}	86.43(4)	95.34(3)
Cl1–M1–Cl1^{i}	180	180
S1–M1–Cl1	93.57(4)	84.66(3)
S1–M1–S1^{i}	180	180
C5–N1–C4	118.1(4)	121.7(4)
C5–N1–C2	118.1(4)	119.2(4)
C4–N1–C2	117.6(4)	118.2(3)
M1[a]–S1–C1–C2	60.89	172.48
M1[a]–S1–C3–C4	59.80	167.98

[a] M = Pt in **1**; M = Pd in **2**.
i = 1 – x, 1 – y, 1 – z in **1**;
i = 1 – x, – y, 1 – z in **2**

Table S4. Results of energy calculations for C–H/Cl–M, C–H/S–M, C–H/M and C–H/N≡C interactions (M = Pd, Pt) at *wb97xd/6-31+g** +lanl2dz* level of theory. Energies are expressed in kcal/mol.

d	**C–H/ Cl–Pd**	**C–H/ Cl–Pt**	**C–H/ S–Pd**	**C–H/ S–Pt**	**C–H/ Pd**	**C–H/ Pt**	**C–H/NC (Pd)**	**C–H/NC (Pt)**
2.50	0.09	0.06	0.85	0.56	–2.21	–1.82	–0.39	–0.39
2.70	–0.42	–0.44	–0.20	–0.44	–2.78	–2.70	–0.56	–0.56
2.80	–0.54	–0.55	–0.47	–0.69	–2.84	–2.88	–0.57	–0.57
2.90	–0.59	–0.60	–0.63	–0.83	–2.80	–2.95	–0.56	–0.56
3.00	–0.60	–0.62	–0.72	–0.90	–2.71	–2.93	–0.54	–0.54
3.20	–0.58	–0.59	–0.75	–0.90	–2.43	–2.72	–0.48	–0.48
3.50	–0.46	–0.49	–0.65	–0.76	–1.92	–2.21	–0.39	–0.39

Table S5. C–H/M interactions obtained from the periodic calculations of axial and equatorially coordinated Pd and Pt.

Complex	Number of C–H/M interactions	C–H/M distances (Å)
2	4	3.785, 4.050, 4.481, 4.933
1	5	3.326, 3.955, 4.798, 4.863, 5.892
2-ax	5	3.719, 4.681, 4.683, 5.164, 5.643
1-eq	4	3.682, 4.058, 4.478, 4.974

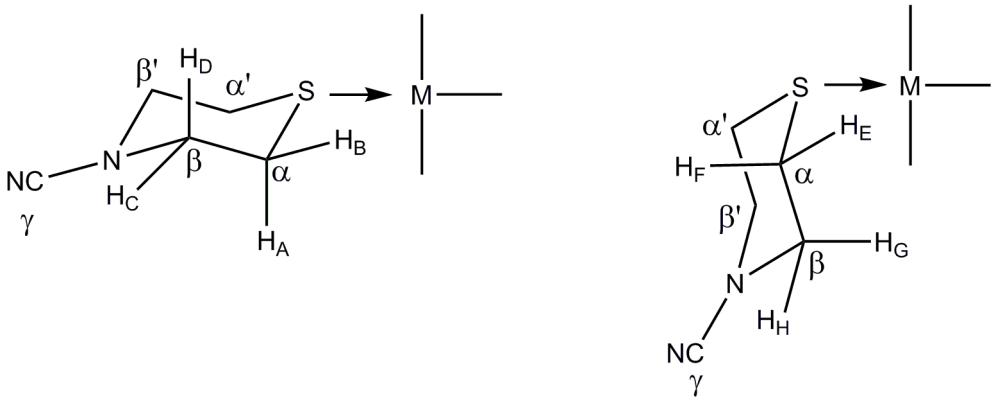

M-eq **M-ax**

Scheme S1. Labelling of atoms used for NMR signal assignments. M = Pt in **1**; M = Pd in **2**.

Table S6. ^{1}H NMR spectral data (399.74 MHz) in DMSO-*d*$_6$ and CD_3NO_2 at 298 K for TM-CN and complexes **1** and **2**.

	DMSO-*d*$_6$	CD_3NO_2
TM-CN	δ 3.40 – 3.36 (m, 4H, $C^{\beta}H_2$ = $C^{\beta'}H_2$), 2.64 (dd, J = 6.2, 3.9 Hz, 4H, $C^{\alpha}H_2$ = $C^{\alpha'}H_2$).	δ 3.47 – 3.39 (m, 4H, $C^{\beta}H_2$ = $C^{\beta'}H_2$), 2.70 (dd, J = 6.2, 3.9 Hz, 4H, $C^{\alpha}H_2$ = $C^{\alpha'}H_2$).
1	**1-ax** (minor): δ 3.75 (br. d, J = 12.1 Hz, 2H, $C^{\beta}H_D$ = $C^{\beta'}H_{D'}$), 3.50 (br. s, 2H, $C^{\beta}H_C$ = $C^{\beta'}H_{C'}$), 3.46 (br. s, 2H, $C^{\alpha}H_B$ = $C^{\alpha'}H_{B'}$), 3.06 (br. d, J = 10.9 Hz, 1H, $C^{\alpha}H_A$ = $C^{\alpha'}H_{A'}$).	**1-ax** (major): δ 3.93 (m, $C^{\beta}H_D$ = $C^{\beta'}H_{D'}$), 3.56 (d, J = 14.9 Hz, $C^{\beta}H_C$ = $C^{\beta'}H_{C'}$), 3.50 (d, J = 12.1 Hz, $C^{\alpha}H_B$ = $C^{\alpha'}H_{B'}$), 3.01 (m, $C^{\alpha}H_A$ = $C^{\alpha'}H_{A'}$).
	TM-CN (major): δ 3.38 (m, 4H, $C^{\beta}H_2$ = $C^{\beta'}H_2$), 2.63 (m, 4H, $C^{\alpha}H_2$ = $C^{\alpha'}H_2$).	**1-eq** (minor): δ 3.77 (d, $C^{\beta}H_C$ = $C^{\beta'}H_{C'}$), 3.67 (m, $C^{\alpha}H_A$ = $C^{\alpha'}H_{A'}$), 3.56 (ovlp., $C^{\beta}H_D$ = $C^{\beta'}H_{D'}$), 3.07 (ovlp, $C^{\alpha}H_B$ = $C^{\alpha'}H_{B'}$).
2	δ 3.52 (br. s, 4H, $C^{\alpha}H_2$ = $C^{\alpha'}H_2$), 2.80 (br. s, 4H, $C^{\alpha}H_2$ = $C^{\alpha'}H_2$)	δ 3.76 (br. s, 4H, $C^{\alpha}H_2$ = $C^{\alpha'}H_2$), 3.18 (br. s, 4H, $C^{\alpha}H_2$ = $C^{\alpha'}H_2$)

Table S7. ^{13}C NMR spectral data (100.53 MHz) in DMSO-d_6 and CD_3NO_2 at 298 K for TM-CN and complexes **1** and **2**.

	DMSO-d_6	CD_3NO_2
TM-CN	δ 117.91 (C^{γ}), 50.68 (C^{β} = $C^{\beta'}$), 25.84 (C^{α} = $C^{\alpha'}$).	δ 117.47 (C^{γ}), 50.67 (C^{β} = $C^{\beta'}$), 25.56 (C^{α} = $C^{\alpha'}$).
1	**1-ax**: δ 116.98 (C^{γ}), 48.80 (C^{β} = $C^{\beta'}$), 31.79 (C^{α} = $C^{\alpha'}$).	**1-ax** (major): δ 116.65 (C^{γ}), 48.39 (C^{β} = $C^{\beta'}$), 28.93 (C^{α} = $C^{\alpha'}$).
	TM-CN: δ 117.96 (C^{γ}), 50.68 (C^{β} = $C^{\beta'}$), 25.70 (C^{α} = $C^{\alpha'}$).	**1-eq** (minor): δ 116.61 (C^{γ}), 48.83 (C^{β} = $C^{\beta'}$), 30.89 (C^{α} = $C^{\alpha'}$).
2	δ 117.48 (C^{γ}), 49.99 (C^{β} = $C^{\beta'}$), 27.46 (C^{α} = $C^{\alpha'}$).	δ 116.65 (C^{γ}), 49.29 (C^{β} = $C^{\beta'}$), 29.76 (C^{α} = $C^{\alpha'}$).